Modern Pathology (2008) 21, 1451–1460

www.modernpathology.org

Absence of *TMPRSS2:ERG* fusions and *PTEN* losses in prostate cancer is associated with a favorable outcome

Maisa Yoshimoto[1], Anthony M Joshua[1], Isabela W Cunha[2], Renata A Coudry[2], Francisco P Fonseca[3], Olga Ludkovski[1], Maria Zielenska[4], Fernando A Soares[2] and Jeremy A Squire[1,5]

[1]*Division of Applied Molecular Oncology, Ontario Cancer Institute, Toronto, ON, Canada;* [2]*Department of Pathology, Hospital do Câncer, São Paulo, Brazil;* [3]*Department of Pelvic Surgery, Hospital do Câncer, São Paulo, Brazil;* [4]*Department of Pathology and Laboratory Medicine, The Hospital for Sick Children, Toronto, ON, Canada and* [5]*Department of Medical Biophysics, Faculty of Medicine, University of Toronto, Toronto, ON, Canada*

***TMPRSS2*:*ERG* gene fusions and *PTEN* deletions are the most common genomic aberrations in prostate cancer. Recent work has suggested that the *TMPRSS2*:*ERG* fusion is associated with a more aggressive phenotype. Similarly, *PTEN* deletion has been associated with biochemical recurrence and lymph node metastasis. To date, there has been no systematic analysis of the combined influence of genomic *PTEN* deletion with *TMPRSS2:ERG* gene fusions on clinical parameters of prostate cancer progression. We carried out a retrospective analysis of 125 prostate cancers with known clinical outcome using interphase fluorescence *in situ* hybridization to detect the relative prevalence of *TMPRSS2:ERG* rearrangements and/or *PTEN* genomic deletions. *TMPRSS2:ERG* rearrangement was found in 60 of 125 (48%) prostate cancers. Duplication of *TMPRSS2:ERG* fusion was observed in seven (6%) tumors. Gleason grade ($P=0.0002$)/score ($P=0.001$), median tumor volume ($P=0.0024$), preoperative PSA ($P=0.001$) and perineural invasion ($P=0.0304$) were significantly associated with biochemical recurrence by univariate analysis with *TMPRSS2:ERG* approaching significance ($P=0.0523$). By multivariate analysis, relevant factors associated with recurrence were Gleason scores 7 ($P=0.001$) and 8–10 ($P=0.015$), *PTEN* homozygous deletion ($P=0.013$) and concurrent *TMPRSS2*:*ERG* fusion and *PTEN* deletion ($P=0.036$). Kaplan–Meier analysis indicated that the presence of *TMPRSS2:ERG* fusion was marginally less favorable in comparison to no fusion. Duplication of fusion gene showed worse prognosis. It was possible to determine the relative frequencies of *PTEN* deletion and/or *TMPRSS2:ERG* fusions in 82 of 125 prostate cancers. With biochemical recurrence as an endpoint, the genomic biomarkers identified three patient groups: (1) 'poor genomic grade' characterized by both *PTEN* deletion and *TMPRSS2:ERG* fusions (23/82, 28%); (2) 'intermediate genomic grade' with either *PTEN* deletion or *TMPRSS2:ERG* fusion (35/82, 43%) and (3) 'favorable genomic grade' in which neither rearrangement was present (24/82, 29%). Kaplan–Meier and multivariate analysis indicate that *TMPRSS2*:*ERG* fusion and *PTEN* loss together are a predictor of earlier biochemical recurrence of disease.**
Modern Pathology (2008) **21,** 1451–1460; doi:10.1038/modpathol.2008.96; published online 23 May 2008

Keywords: interphase FISH; *PTEN* haploinsufficiency; prognosis; biomarker; biochemical recurrence

The identification of prognostic molecular biomarkers is recognized as critically important in the future clinical management of prostate cancer. Despite the clinical utility of Gleason score, pathological stage and serum PSA in assessing prognosis and guiding management, further molecular determinants are needed that more accurately address pathways that underlie tumorigenesis of prostate cancer.[1]

Chromosomal deletions of 10q suggested that the phosphatase and tensin homologue (*PTEN*) gene at cytoband 10q23.3 is strongly associated with the progression of prostate cancer.[2–4] PTEN plays an important role in the modulation of the phosphatidylinositol-3-kinase (PI3K) pathway by catalyzing degradation of phosphatidylinositol-(3,4,5)-triphosphate (PIP3) generated by PI3K.[5] PIP3 activates the protein kinase AKT which then modulates a number of downstream targets with important roles in apoptosis and the cell-cycle progression, including *BAD*,[6] *CASP3* and *CASP9*,[7] *MDM2*,[8] *mTOR*,[9] *FKHR*[10] and *FOXO3A*,[11] *p27*[12] and the recently recognized

Correspondence: Dr JA Squire, PhD, Division of Applied Molecular Oncology, Ontario Cancer Institute, Princess Margaret Hospital, 610 University Avenue, Room 9-721, Toronto, ON M5G 2M9 Canada.
E-mail: jeremy.squire@utoronto.ca
Received 14 March 2008; revised 25 April 2008; accepted 26 April 2008; published online 23 May 2008

JNK pathway.[13] *PTEN* deletion is associated with tumor progression[14–16] and more predictive of shorter time to biochemical recurrence of disease,[17] emphasizing the crucial role of *PTEN* as marker of tumor behavior in prostate cancer.

The discovery of recurrent translocations in ~40–60% of prostate carcinoma,[4,18–24] involving the *TMPRSS2* gene at 21q22.3 with members of the erythroblast transformation specific (*ETS*) transcription factor family, such as *ERG* (21q22.2), *ETV1* (7p21.2), *ETV4* (17q21) or *ETV5* (3q28) genes, has provided new insights into prostatic carcinogenesis. Although the downstream molecular pathways of *ETS* fusion genes are only beginning to be clarified, clinical associations have been reported in early studies.[19,22,25–28] For instance, *TMPRSS2:ERG*-rearranged prostate cancers have been associated with a greater likelihood of lethal prostate cancer,[26,27] moderate to poorly differentiated tumors[25] and higher stage diseases with pelvic lymph node metastases.[19] Evidence of specific *TMPRSS2:ERG* isoforms were also described to be associated with high levels of fusion mRNA expression and early biochemical recurrence following radical prostatectomy.[22] However, there are a number of conflicting studies[29,30] about the prognostic importance of the gene fusion; so the clinical significance of *TMPRSS2:ERG* fusions remains to be clarified.

Given the potential of both *TMPRSS2:ERG* fusions and *PTEN* genomic deletions to contribute to prognosis prediction in prostate cancer, additional genotype–phenotype correlation studies will be helpful. In addition, it is unclear whether the *TMPRSS2:ERG* rearrangements may be accompanied by *PTEN* genomic loss, or in contrast, these are mutually exclusive events. There has been no systematic analysis to date of the frequency at which *PTEN* and *TMPRSS2:ERG* rearrangements occur simultaneously in prostate cancer, or to examine clinical phenotypes associated with genomic mutations affecting both pathways. Therefore, this study was designed to retrospectively assess the overall frequency and clinical impact of *TMPRSS2:ERG* rearrangements using a clinically-annotated tissue microarray. We also provide the results of clinical impact of cooperation between *TMPRSS2:ERG* gene rearrangements and *PTEN* genomic deletion in prostate cancer samples that became available after the publication of our previous study.[17] Our results further implicate *TMPRSS2:ERG* rearrangements as a prognostic value in the primary tumor, in addition to providing insights into prostate cancer pathophysiology.

Materials and methods

Tissue Specimens

The collection of all tissue specimens, clinical and patient follow-up data was obtained after informed consent in accordance with the Hospital do Câncer Research Ethics guidelines (São Paulo, Brazil). Archival formalin-fixed, paraffin-embedded tissues were obtained from 125 radical prostatectomies performed between 1997 and 2000 at the Hospital do Câncer, AC Camargo, São Paulo, Brazil. For control purposes, 10 non-neoplastic prostate tissue samples were obtained from patients undergoing surgery solely for benign prostate hyperplasia. The prostate cancer cohort and control specimens were sampled using a 0.6-mm diameter tissue core distributed on tissue microarray slide. Adjacent hematoxylin and eosin (H&E) stained section was reviewed by two pathologists to determine the presence and extent of morphologically representative areas of the original tumors in each tissue core. Reassessment of Gleason grading in a contiguous H&E stained tissue microarray section assured the presence of prostate adenocarcinoma and the fidelity of the intended tissue microarray core. The size of tumor was based on assessment of total surface area of gland examined histologically involved by carcinoma. Preoperative PSA level was available for all patients and the PSA nonfailure was defined as PSA remaining below 0.2 ng/ml after radical prostatectomy.

Fluorescence *In Situ* Hybridization

Break-apart fluorescence *in situ* hybridization (FISH) was used for studying the *TMPRSS2*:*ERG* gene rearrangement as previously described.[31] The following bacterial artificial chromosome (BAC) clones were used. BACs located at: (a) the 3′ *ERG* gene locus (RP11-476D17, 3′*ERG* sequence extending inward past exon 4), (b) the 5′ *ERG* gene locus (RP11-95I21, 5′*ERG* sequence extending inward into exon 10), (c) the *TMPRSS2* locus (RP11-535H11) and (d) the telomeric BACs to the 5′ end of *TMPRSS2* locus (RP11-35C4, RP11-891L10 and RP11-260O11, 325 kb downstream from the 5′ end of the *TMPRSS2* gene; Figure 1a). The BAC clones were obtained from The Center for Applied Genomics (Toronto, Canada). DNA was extracted and labeled with SpectrumGreen-dUTP, SpectrumOrange-dUTP (Vysis Inc., Downers Grove, IL, USA) or diethylaminocoumarin (DEAC)-dUTP (PerkinElmer Life and Analytical Sciences, Boston, MA, USA) using the Vysis nick-translation kit according to manufacturer's instructions (Vysis Inc.). The integrity and correct chromosome localization of all BAC clones were verified by hybridization to metaphase spreads of normal peripheral lymphocytes.

Sequential dual-color FISH method was applied to the prostate cancer tissue microarray to investigate the occurrence of *PTEN* genomic deletion in addition to *TMPRSS2:ERG* gene rearrangements in 82 of 125 prostate cancer cohort. Dual-color FISH on paraffin-embedded tissue microarray tissue was performed using commercially available DNA probes for cytoband 10q23 (Spectrum

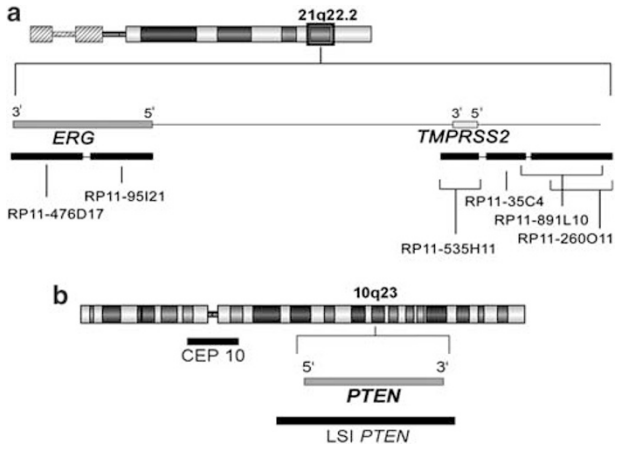

Figure 1 FISH probes used to detect the genomic alteration in prostate cancer. (**a**) Location and names of the BAC probes spanning the genomic region of the *ERG* and *TMPRSS2* loci at chromosome 21q22.2 and. The linear order and approximate distances of the BAC clones are based on the Human March 2006 assembly of the UCSC Genome Browser. (**b**) Genomic localization of the commercially available locus-specific *PTEN* probe and α-satellite DNA sequences of chromosome 10 probe (Vysis Inc.).

Orange *PTEN* locus-specific probe) and region 10p11.1-q11.1 (Spectrum Green centromere of chromosome 10 probe) (LSI *PTEN*/CEP 10; Vysis Inc.). The *PTEN* genomic probe spans 368 kb and starts 166 kb from 5′ end of the gene and extends 98 kb past the 3′ end of the gene (Figure 1b). Histologic tissue microarray tissue sections (5 μm) were deparaffinized with a series of xylene prior to immersion in 100% ethanol. FISH was carried out as described.[17]

Data Analysis

The *TMPRSS2*:*ERG* fusion was evaluated for each probe by spot visualization and enumeration in a range from 50 to 100 nonoverlapped, intact interphase nuclei per tumor tissue core using a Zeiss Imager.Z1 microscope equipped with a digital camera AxioCam MRm and AxioVision 4.3 capturing software (Carl Zeiss Canada Ltd, Canada). The *ERG* rearrangement in tumor nuclei was detected by either the split of one of the colocalized 3′ and 5′ *ERG* signals in addition to a fused signal of the unaffected chromosome 21 or the hemizygous loss of 5′ *ERG* (RP11-95I21—green signal), whereas the homologue signal colocalized to the fused signal of the apparently unaffected loci at chromosome 21. The telomeric BACs to the 5′ end of *TMPRSS2* locus signal colocalized with the signal of the 3′ *ERG* BAC, confirming the presence of the typical 5′ *TMPRSS2*:3′ *ERG* rearrangements. When the BAC telomeric to the 5′ end of *TMPRSS2* (blue signal) was well separated from the 3′ *ERG* BAC (red signal), the *TMPRSS2*:*ERG* rearrangement was confirmed using the *TMPRSS2* BAC (RP11-535H11—blue), 5′ *ERG* (RP11-95I21—green) and 3′ *ERG* BAC (RP11-476D17—red). Based on hybridization in 10 control cores (data not shown) and tumor cohort, the detection of *TMPRSS2*:*ERG* rearrangement was defined as cutoff >10% when the distance between signals was >3 times the estimated signal diameter.[32]

PTEN copy number was evaluated for each probe by counting spots in a range from 50 to 100 nonoverlapped, intact interphase nuclei per tumor tissue core. Based on hybridization in 10 control cores (data not shown), hemizygous deletion of *PTEN* were defined as >20% (mean + 3 s.d. in non-neoplastic controls) of tumor nuclei containing one *PTEN* locus signal and by the presence of CEP 10 signals. Homozygous deletion of *PTEN* was exhibited by the simultaneous lack of the both *PTEN* locus signals and by the presence of control signals[32–35] in >30% of cells.[33]

Statistical Analysis

FISH findings for *TMPRSS2*:*ERG* fusion were correlated in a univariate and multivariate fashion with clinical and pathologic measures of disease aggressiveness. A comprehensive description of the clinical parameters associated with the adenocarcinomas having the *TMPRSS2:ERG* fusion is summarized in Table 1. Frequency of *TMPRSS2*:*ERG* rearrangements was also correlated with *PTEN* genomic deletion in addition to determinants of disease mortality and morbidity, such as PSA, and extraprostatic extension and time to biochemical relapse. Univariate and multivariate analyses of risk of biochemical failure were studied by Cox proportional hazard model. A significant correlation between two parameters was taken at the 95% confidence interval. *P*-values <0.05 were considered significant. The survival rate was estimated by applying the Kaplan–Meier method. The endpoint for calculating the survival time was defined by time from radical prostatectomy until the occurrence of metastasis or PSA determined biochemical recurrence, ie the date of first PSA increase above 0.2 ng/ml. (median follow-up time 87.4 months, range 11.5–161.6). All calculations were performed using Stata 9.1 (StataCorp LP).

Results

TMPRSS2:ERG Fusion

A total of 125 archival tissues with anonymous clinical annotation were analyzed for *TMPRSS2:ERG* rearrangements by interphase tricolor FISH. *TMPRSS2:ERG* rearrangement was found in 60 of 125 (48%) prostatic adenocarcinomas samples. There was evidence of *TMPRSS2:ERG* fusion with deletion of 5′ *ERG* probe in 43 of 125 (34%) cases. As previously characterized,[31] sequential FISH analysis using the BAC set telomeric to the 5′ end of *TMPRSS2* (RP11-35C4, RP11-891L10 and

Table 1 Clinicopathological parameters from 122 of the 125 prostatic adenocarcinoma patients

Clinicopathological parameters	*Number of cases*	TMPRSS2:ERG		P-*value*
		Not fused	*Fusion*	
Preoperative PSA (ng/ml)[a]				0.612
0.9–4.0	9	3 (33.33)	6 (66.67)	
4.0–10.0	58	31 (53.45)	27 (46.55)	
10.1–20.0	37	21 (56.76)	16 (43.24)	
20.1–84.0	15	7 (46.67)	8 (53.33)	
Median tumor volume (%)[a]				0.886
0–10.0	35	19 (54.29)	16 (45.71)	
10.1–20.0	28	14 (50.00)	14 (50.00)	
20.1–85.0	49	24 (48.98)	25 (51.02)	
Gleason score				0.636
4–6	74	39 (52.70)	35 (47.30)	
7	35	18 (51.43)	17 (48.57)	
8–9	13	5 (38.46)	8 (61.54)	
Pathologic stage				0.966
pT2a	10	6 (60.00)	4 (40.00)	
pT2b	58	30 (51.72)	28 (48.28)	
pT3a	39	19 (48.72)	20 (51.28)	
pT3b	9	4 (44.44)	5 (55.56)	
pT4	6	3 (50.00)	3 (50.00)	
Seminal vesicle invasion[a]				0.337
Negative	108	54 (50.00)	54 (50.00)	
Positive	9	6 (66.67)	3 (33.33)	
Perineural infiltration				0.344
Negative	18	11 (61.11)	7 (38.89)	
Positive	104	51 (49.04)	53 (50.96)	
Angiolymphatic invasion[a]				0.400
Negative	89	43 (48.31)	46 (80.70)	
Positive	26	15 (57.69)	11 (19.30)	
Capsular invasion[a]				0.387
Negative	52	29 (55.77)	23 (44.23)	
Positive	69	33 (47.83)	36 (52.17)	
Extraprostatic extension[a]				0.835
Negative	92	46 (50.00)	50 (50.00)	
Positive	19	9 (47.37)	10 (52.63)	
Lymphonodal invasion[a]				0.154
Negative	108	53 (49.07)	55 (50.93)	
Positive	2	2 (100.00)	0 (0.00)	
Biochemical recurrence				0.047
Negative	62	37 (59.68)	25 (40.32)	
Positive	60	25 (41.67)	35 (58.33)	

[a]Values not available for all 122 cases.
The three atypical cases were excluded from the clinicopathological correlation analysis given that complex genomic rearrangement involving an unknown chromosomal partner(s) could not be elucidated as previously described.
Median overall survival was 87.4 months (11.5–161.6).
Values in parentheses indicate the percentage of sample in each category.
P-value = χ^2-analysis.

RP11-260O11—blue) identified a split of the typical colocalized 5′ end of *TMPRSS2*:*3′ ERG* probe signals in 3 of these 43 samples. This is indicative of a more complex genomic alteration, involving an unknown chromosomal partner(s). Confirmation of the *TMPRSS2:ERG* fusion in these three samples showing the atypical FISH pattern was obtained by the BAC set consisting of the 3′ *ERG* BAC (RP11-476D17), 5′ *ERG* (RP11-95I21) and the *TMPRSS2* locus (RP11-535H11). Interestingly, an extra copy of *TMPRSS2:ERG* fusion associated with deletion of 5′ *ERG* probe was observed in 7 of the 43 samples showing *TMPRSS2:ERG* fusion with deletion of 5′ *ERG* (Table 2). There was evidence of FISH

Table 2 Summary of the *TMPRSS2:ERG* fusion status by tri-color FISH

TMPRSS2:ERG *status*	*Number of cases (%)*
TMPRSS2:ERG fusion via translocation	17 (14%)
TMPRSS2:ERG fusion via genomic deletion of 5' *ERG*	43 (34%)[a]
Other rearrangements	3 (2.4%)
Not fused	62 (49.6%)
Total	125

[a]Duplication of *TMPRSS2:ERG* fusion was observed in 7 of the 43 samples showing *TMPRSS2:ERG* fusion via genomic deletion of the 5′ end of the *ERG* gene.

TMPRSS2:ERG fusion with no deletion of 5′ *ERG* probe in 17 of 125 (14%) cases. Only 1 of the 17 cases showed the BAC set telomeric to the 5′ end of *TMPRSS2* (RP11-35C4, RP11-891L10 and RP11-260O11—blue) well separated from the 3′ *ERG* BAC (RP11-476D17—red) (Table 2).

In addition to the 60 *TMPRSS2:ERG* fused cases, 3 atypical cases had abnormal *TMPRSS2*:*ERG* FISH colocalization pattern. The 3′ *ERG* RP11-476D17 (red signal) did remain juxtaposed to the 5′ *ERG* RP11-95I21 (green signal), but failed to exhibit the expected colocalization of the *TMPRSS2* locus (RP11-535H11—blue) with the *ERG* gene probes. We were not able to detect FISH fusions between *TMPRSS2* and *ETV1* or *ETV4* in any of these three cases with abnormal FISH *TMPRSS2:ERG* break-apart results. Furthermore, extra copies of the *TMPRSS2* locus (RP11-535H11—blue) were observed in the atypical samples. Such findings indicate that: (a) fusion events between *TMPRSS2* and other genes are possible and (b) *TMPRSS2*:*ERG* fusions may sometimes have concurrent complex genomic rearrangements within the ~2.9 Mb that separates these two genes. However, the three atypical cases were excluded from the clinicopathological correlation analysis given that complex genomic rearrangement involving an unknown chromosomal partner(s) could not be elucidated.

Among the 60 rearranged *TMPRSS2:ERG* tumors detected, the Gleason scores were 4–6 (35 tumors), 7 (17 tumors) and 8–9 (8 tumors). A median tumor volume of >20% was found in 25/60 rearranged *TMPRSS2:ERG* tumors. In addition, early biochemical recurrence was detected in all seven samples with an extra copy of *TMPRSS2:ERG* fusion associated with deletion of 5′ *ERG* probe.

Concomitant Presence of *TMPRSS2:ERG* Fusion and *PTEN* Genomic Deletion

After acquisition of FISH data, the cases were reviewed to search for potential associations between *PTEN* deletion as studied previously,[17] and *TMPRSS2:ERG* rearrangements. Therefore, we examined differential status of *PTEN* (deleted or not deleted) and presence of *TMPRSS2:ERG* fusion in 82 of the 125 tumor samples to assess its utility as biomarker of prognosis. Overall, *PTEN* deletion in addition to the presence of *TMPRSS2:ERG* rearrangement was observed in 23 of 82 (28%) prostatic adenocarcinomas. *PTEN* deletion was also found in 14 prostate adenocarcinoma samples showing absence of *TMPRSS2:ERG* rearrangement (14/82, 17%). There was evidence of no copy change of *PTEN* locus with *TMPRSS2:ERG* fusion in 21 of 82 (26%) cases and no copy change of *PTEN* locus with absence of *TMPRSS2:ERG* fusion in 24 of 82 (29%) cases. The description of the *TMPRSS2:ERG* fusion concomitantly with *PTEN* deletion is summarized in Table 3. A comprehensive description of the clinicopathological parameters associated with 47 adenocarcinomas (23 cases showing both *PTEN* deletion and *TMPRSS2:ERG* fusion, and 24 cases in which neither rearrangement was present) is summarized in Table 4. Representative images of *TMPRSS2:ERG* rearrangement and *PTEN* deletion are shown in Figure 2.

Table 3 Distribution of samples showing *TMPRSS2:ERG* fusion and *PTEN* deletion in 82 prostatic adenocarcinomas

	TMPRSS2:ERG *fusion*	*No fusion*
PTEN deletion	23 (28%)	14 (17%)
PTEN not deleted	21 (26%)	24 (29%)

Statistical Analysis of Clinical Parameters and Genomic Alterations

High Gleason score and clinical parameters of aggressive disease such as extraprostatic extension ($P=0.0002$), seminal vesicle invasion ($P=0.0023$), margin status ($P=0.0008$), neoadjuvant hormone therapy ($P=0.0004$), Gleason grade ($P=0.0002$)/score ($P=0.001$), median tumor volume ($P=0.0024$), preoperative PSA ($P=0.001$), *PTEN* deletion ($P=0.009$), concurrent *TMPRSS2*:*ERG* fusion and *PTEN* deletion (0.001) and perineural invasion ($P=0.0304$) were significantly associated with biochemical recurrence by univariate analysis with *TMPRSS2:ERG* approaching significance ($P=0.0523$; Table 5). By multivariate analysis, relevant factors to explain biochemical failure included Gleason score (7 and 8–10, $P=0.001$ and $P=0.015$, respectively), concurrent *TMPRSS2:ERG* fusion and *PTEN* deletion (0.036) and *PTEN* homozygous deletion (0.013). The *PTEN* findings reflect those previously reported for this cohort[17] (Table 6). For comparison purpose, Kaplan–Meier survival analysis applying established clinical markers, such

Table 4 Clinicopathological parameters from 47 of the 82 prostatic adenocarcinoma patients analyzed for the differential status of *PTEN* (deleted or not deleted) and presence of *TMPRSS2:ERG* fusions

	TMPRSS2:ERG *fusion and* PTEN *deletion*	TMPRSS2:ERG *not fused and* PTEN *not deleted*	P-*value*
Preoperative PSA (ng/ml)[a]			0.638
0.9–4.0	1	0	
4.0–10.0	10	14	
10.1–20.0	6	7	
20.1–84.0	4	3	
Median tumor volume (%)[a]			0.309
0–10.0	4	10	
10.1–20.0	5	6	
20.1–85.0	13	11	
Gleason score			0.308
4–6	12	16	
7	7	7	
8–9	4	1	
Pathologic stage			0.743
pT2a	1	1	
pT2b	12	11	
pT3a	6	9	
pT3b	3	1	
pT4	1	2	
Seminal vesicle invasion[a]			0.847
Negative	18	22	
Positive	2	2	
Perineural infiltration			0.242
Negative	2	5	
Positive	21	19	
Angiolymphatic invasion[a]			0.129
Negative	17	17	
Positive	5	5	
Extraprostatic extension			0.587
Negative	17	16	
Positive	6	8	
Lymphonodal invasion[a]			0.947
Negative	21	20	
Positive	1	1	

[a]Values not available for all 47 samples.
Median overall survival was 109 months (49.3–161.3).
P-value = χ^2-analysis.

as the preoperative PSA, seminal vesicle invasion and surgical margins status, was considered to identify subgroups with different prognosis with respect to time to relapse after surgery. The estimated disease-free survival curves demonstrated association between *TMPRSS2:ERG* fusion and short time based on PSA recurrence intervals (Figure 3a). Significantly, the occurrence of duplication of the *TMPRSS2:ERG* fusion was associated with a much earlier onset of biochemical recurrence based on PSA values (Figure 3b). Furthermore, the estimated disease-free survival curves demonstrated considerable association of coexisting *PTEN* deletion and *TMPRSS2:ERG* rearrangements with short time based on PSA recurrence intervals (Figure 3c). This analysis allowed for three broad groupings of differential patient outcome based on time to biochemical recurrence: (1) a poor prognostic group characterized by both *PTEN* deletion and *TMPRSS2:ERG* fusions; (2) an intermediate group with either *PTEN* deletion or *TMPRSS2:ERG* fusion and (3) a favorable prognostic group with neither event.

Discussion

The search for accurate biomarkers in prostate cancer is critical for evolution of accurate management of prostate cancer. This study evaluated the two leading genomic biomarkers (*PTEN* deletion and *TMPRSS2:ERG* rearrangements) for their contribution to prostate cancer prognosis in a large Brazilian cohort. Figure 3c illustrates the two

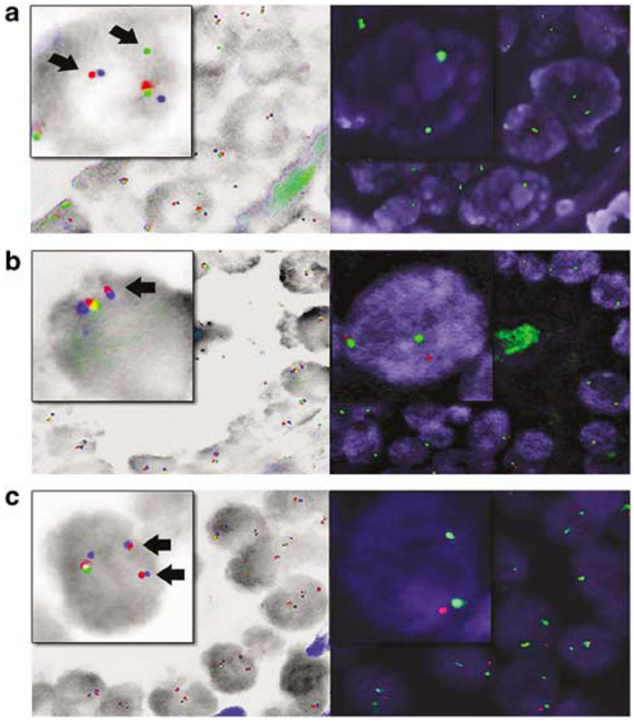

Figure 2 Different patterns of genomic alterations detected by interphase FISH in prostate cancer. (**a–c**) Representative FISH images are shown for prostate cancer tissue microarray applying the *TMPRSS2:ERG* (left panel) and *PTEN* (right panel) probes. The left panel shows a representative pseudo-color image with the inverted-DAPI counterstained nuclei as a gray tone overlay to facilitate interpretation. The right panel shows a representative pseudo-color image with the DAPI counterstained nuclei. The rectangles show a enlarged nucleus FISH image. (**a**) Representative break-apart tri-color FISH strategy identifies the 5′ *ERG* BAC (RP11-95I21—green) well separated from the 3′*ERG* BAC (RP11-476D17—red) (arrow). The fused signal of the 3′ *ERG* (red) and *TMPRSS2* gene locus (blue) that confirms the *TMPRSS2:ERG* fusion is arrowed used to detect *TMPRSS2:ERG* fusions (arrows). The BAC probes hybridizing to the unaffected *TMPRSS2:ERG* locus show the normal red-green (yellow) and blue colocalization pattern. This extreme nuclear separation is indicative of *TMPRSS2:ERG* rearrangements via genomic translocation mechanisms. Representative *PTEN* FISH image of homozygous deletion in prostate cancer shows absence of red signal for 10q23/*PTEN* locus in most of the nuclei and retained green signals for CEP 10. (**b**) The fused signal of the 3′ *ERG* (red) and *TMPRSS2* gene locus (blue) that confirms the *TMPRSS2:ERG* fusion is arrowed. In addition, the hemizygous loss of 5′ *ERG* BAC (green) indicates an intervening genomic microdeletion of chromosome 21. The BAC probes hybridizing to the unaffected *TMPRSS:ERG* locus show the normal tri-color (red, green and blue) colocalization pattern. Representative *PTEN* FISH image of two signals of both red signals (10q23/*PTEN* locus) and green signals (CEP 10) in most of the nuclei indicating no deletion of *PTEN* in tumor cells. (**c**) Duplication of the fused signal of the 3′ *ERG* (red) and *TMPRSS2* gene locus (blue) that confirms the *TMPRSS2:ERG* fusion is arrowed. In addition, the hemizygous loss of 5′ *ERG* BAC (green) indicates an intervening genomic microdeletion of chromosome 21. The BAC probes hybridizing to the unaffected *TMPRSS:ERG* locus show the normal tri-color (red, green and blue) colocalization pattern. The *PTEN* FISH image shows tumor cells with single red signal for 10q23/*PTEN* locus in most of the nuclei and paired green signals for CEP 10 indicating hemizygous deletion of 10q23/*PTEN* locus in prostate cancer.

genomic biomarkers (*TMPRSS2:ERG* fusion and *PTEN* deletion) which appeared to segregate prostate cancer cases into three broad groupings based on biochemical recurrence as an endpoint: (1) 'poor genomic grade' characterized by both *PTEN* deletion and *TMPRSS2:ERG* fusions; (2) 'intermediate genomic grade' with either *PTEN* deletion or *TMPRSS2:ERG* fusion and (3) 'favorable genomic grade' in which neither rearrangement was present. Our findings reinforce previous studies that examined each of these promising biomarkers individually and add hypotheses about their interactions in prostatic carcinogenesis.

The proportion of prostatic adenocarcinoma samples with *TMPRSS2:ERG* rearrangement (48%) is in agreement with similar cohorts enclosing diverse stage and Gleason scores[19,22] whereas subsets with earlier stage disease tend to have lower incidence.[26,27] This association of the gene rearrangement with more advanced disease has been suggested previously.[36] Indeed several large cohorts have suggested an adverse prognostic impact of the *ETS* fusion genes with both pathological[19,28] and overall survival endpoints.[26,27] The confirmation of the finding of poorest prognosis associated with the duplication of gene fusion via 5′ *ERG* deletion variant also likely highlight important aspects of the pathophysiology of prostate cancer. The effective double dose of *ERG* gene alteration associated with this variant is likely to lead to an increased rate of biochemical recurrence seen in our and other cohorts.[26,37,38] Collectively, our data indicates that the duplication of gene fusion via 5′ *ERG* deletion variant is predictive of a shorter time to biochemical recurrence of disease. However, some authors have suggested that duplication of the fusion may be a manifestation of general polyploidy rather than a specific duplication event.[39]

As *PTEN* deletion and *TMPRSS2:ERG* abnormalities could be additive or mutually exclusive, we evaluated the prognostic information gained by *TMPRSS2:ERG* analysis alone and in combination with genomic *PTEN* deletions. The additive effect seen may relate to increased cellular motility, a phenotype that can be attributable to both *ETS* fusion[40] and *PTEN* deletion.[41,42] Thus together, activation of these pathways may facilitate epithelial–mesenchymal transition that is characteristic of malignant transformation.[43]

To further explore the potential for synergy between these genomic events, we used Oncomine[44] to interrogate two publicly available microarray studies of prostate cancer progression for differentially expressed genes between *ETS* overexpressing and nonoverexpressing prostate cancers.[45,46] The *ETS* overexpressing prostate cancers demonstrated dysregulation of genes particularly involved in the Wnt pathway. *PTEN* deletion and its sequel are also likely to affect the same pathways and synergize with the consequences of *ETS*-related overexpression. Akt activation is also known to inhibit

Table 5 Univariate Cox proportional hazard analysis of biochemical failure risks (each variable predictor analyzed separately)

Variables	*Category*	*BRFS*		*HR*	*95% CI*
		5 years	P-*value*		
Perineural invasion	Negative	77.04	0.0304	1.0	Reference
	Positive	49.94		2.91	1.05–8.04
Extraprostatic extension	Negative	63.45	0.0002	1.0	Reference
	Positive	26.78		3.10	1.67–5.76
Margins	Negative	62.99	0.0008	1.0	Reference
	Positive	25.70		2.40	1.41–4.07
Seminal vesicle invasion	Negative	57.33	0.0023	1.0	Reference
	Positive	20.00		3.28	1.46–7.36
Neoadjuvant hormonotherapy	Negative	59.49	0.0004	1.0	Reference
	Positive	33.33		1.59	1.21–2.08
Primary gleason grade	2–3	48.01	0.0002	1.0	Reference
	4	15.43		1.48	1.74–6.95
Gleason score	4–6	69.90	<0.001	1.0	Reference
	7	32.58		3.14	1,79–5.49
	8	19.94		3.42	1.63–7.16
Median tumor volume	0–10.0	71.43	0.0024	1.0	Reference
	10.1–20.0	62.95		1.10	0.46–2.60
	20.1–85.0	39.63		2.67	1.35–5.30
Preoperative PSA	0.9–4.0	77.78	<0.001	1.0	Reference
	4.1–10.0	62.85		2.38	0.56–10.08
	10.1–20.0	55.52		2.86	0.66–12.37
	20.1–84.0	6.67		13.08	2.93–58.26
TMPRSS2:*ERG* fusion	Negative	61.77	0.0523	1.0	Reference
	Positive	45.72		1.99	1.21–3.27
PTEN deletion	Negative	57.04	0.0009	1.0	Reference
	Hemizygous	50.00		1.53	0.82–2.85
	Homozygous	0.0		5.93	2.12–16.84
PTEN deletion and *TMPRSS2*:*ERG* fusion	Negative	59.35	0.001	1.0	Reference
	Positive	30.43		2.49	1.43–4.35

BRFS, biochemical recurrence-free survival; CI, confidence interval; HR, hazard ratio.

Table 6 Multivariate model to biochemical failure risks by Cox logistic regression analysis

Variables	*Category*	*HR*	P-*value*	*95% CI*
Gleason score	4–6	1.0		Reference
	7	3.07	<0.001	1.75–5.37
	8–10	2.65	0.015	1.21–5.81
PTEN status	Negative	1.0		Reference
	Hemizygous deletion	1.30	0.433	0.67–2.54
	Homozygous deletion	4.43	0.013	1.36–14.40
PTEN deletion and *TMPRSS2*:*ERG* fusion	Negative	1.0		Reference
	Positive	1.87	0.036	1.04–3.36

CI, confidence interval; HR, hazard ratio.

GSK3β.[3,47] The combination of these two events would theoretically lead to extra translocation of β-catenin to the nucleus further assisting cellular motility and epithelial to mesenchymal transition.[48] Additionally, we observed an upregulation of BRAF in *ETS* overexpressing tumors, such that combined signaling through ERK is also likely to increase cellular migration phenomena.

Our new findings suggests that the subgroup with absence of both *TMPRS2:ERG* and genomic *PTEN* alterations may be designated as favorable genomic grade. Kaplan–Meier and multivariate analysis indicates that *TMPRSS2*:*ERG* fusion and *PTEN* loss together are a predictor of earlier biochemical recurrence of disease. The acquisition of the *TMPRSS2:ERG* fusion and concomitant *PTEN* deletion at an earlier phase in prostatic oncogenesis appear to be an additional determinant of the phenotype that govern a more aggressive tumor phenotype. Further studies should validate this

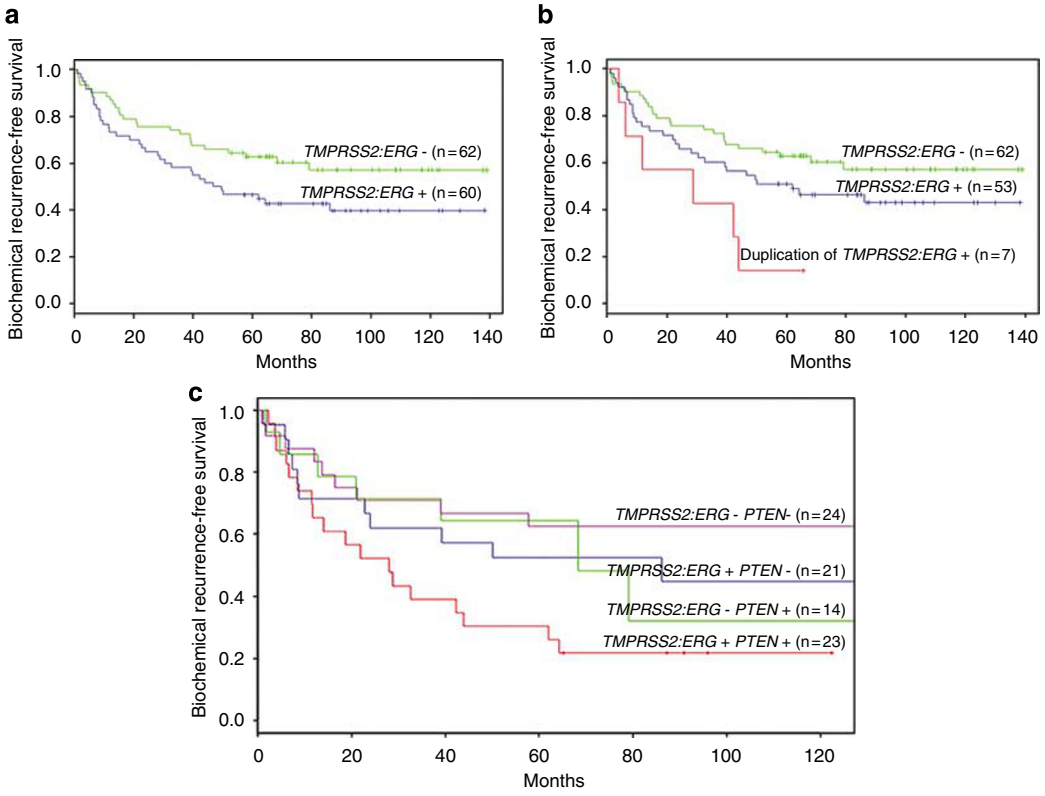

Figure 3 Kaplan–Meier curves illustrating biochemical recurrence-free survival among prostate cancer patients defined by the status of selected clinicopathological parameters, *TMPRSS2:ERG* rearrangements and *PTEN* copy number changes; (+) presence, (−) absence. (**a**) PSA recurrence-free survival curve stratified by the *TMPRSS2:ERG* rearrangements (absence or presence of gene fusion) on 122 prostate cancer patients and (**b**) when duplicate *TMPRSS2:ERG* FISH fusion signals were present (red curve) the outcome was the least favorable. (**c**) PSA recurrence-free survival analysis stratified by *TMPRSS2:ERG* rearrangements and *PTEN* copy number changes on 82 prostate cancer patients.

concept to allow better stratification of care in prostate cancer.

Acknowledgements

We acknowledge the assistance of Dr Arul Chinnaiyan and Dr Scott Tomlins in our Oncomine data analysis. This work has been supported by the Prostate Cancer Research Foundation of Canada (PCRFC), the National Cancer Institute of Canada (NCIC), the Department of Defense Congressionally Directed Medical Research Program Predoctoral Traineeship Award (PC050531) and the American Urological Association Foundation/ Astellas Research Scholar award.

References

1 Joshua AM, Evans A, Van der Kwast T, *et al.* Prostatic preneoplasia and beyond. Biochim Biophys Acta 2008;1785:156–181.
2 Hughes S, Yoshimoto M, Beheshti B, *et al.* The use of whole genome amplification to study chromosomal changes in prostate cancer: insights into genome-wide signature of preneoplasia associated with cancer progression. BMC Genomics 2006;7:65.
3 Yoshimoto M, Cutz JC, Nuin PA, *et al.* Interphase FISH analysis of PTEN in histologic sections shows genomic deletions in 68% of primary prostate cancer and 23% of high-grade prostatic intra-epithelial neoplasias. Cancer Genet Cytogenet 2006;169:128–137.
4 Yoshimoto M, Joshua AM, Chilton-Macneill S, *et al.* Three-color FISH analysis of TMPRSS2/ERG fusions in prostate cancer indicates that genomic microdeletion of chromosome 21 is associated with rearrangement. Neoplasia 2006;8:465–469.
5 Besson A, Robbins SM, Yong VW. PTEN/MMAC1/ TEP1 in signal transduction and tumorigenesis. Eur J Biochem 1999;263:605–611.
6 Datta SR, Dudek H, Tao X, *et al.* Akt phosphorylation of BAD couples survival signals to the cell-intrinsic death machinery. Cell 1997;91:231–241.
7 Cardone MH, Roy N, Stennicke HR, *et al.* Regulation of cell death protease caspase-9 by phosphorylation. Science 1998;282:1318–1321.
8 Ashcroft M, Ludwig RL, Woods DB, *et al.* Phosphorylation of HDM2 by Akt. Oncogene 2002;21:1955–1962.
9 Majumder PK, Febbo PG, Bikoff R, *et al.* mTOR inhibition reverses Akt-dependent prostate intraepithelial neoplasia through regulation of apoptotic and HIF-1-dependent pathways. Nat Med 2004;10:594–601.
10 Brunet A, Bonni A, Zigmond MJ, *et al.* Akt promotes cell survival by phosphorylating and inhibiting a Forkhead transcription factor. Cell 1999;96:857–868.
11 Trotman LC, Alimonti A, Scaglioni PP, *et al.* Identification of a tumour suppressor network opposing nuclear Akt function. Nature 2006;441:523–527.
12 Graff JR, Konicek BW, McNulty AM, *et al.* Increased AKT activity contributes to prostate cancer progression

by dramatically accelerating prostate tumor growth and diminishing p27Kip1 expression. J Biol Chem 2000;275:24500–24505.
13 Vivanco I, Palaskas N, Tran C, *et al.* Identification of the JNK signaling pathway as a functional target of the tumor suppressor PTEN. Cancer Cell 2007;11:555–569.
14 Koksal IT, Dirice E, Yasar D, *et al.* The assessment of PTEN tumor suppressor gene in combination with Gleason scoring and serum PSA to evaluate progression of prostate carcinoma. Urol Oncol 2004;22:307–312.
15 Bertram J, Peacock JW, Fazli L, *et al.* Loss of PTEN is associated with progression to androgen independence. Prostate 2006;66:895–902.
16 Schmitz M, Grignard G, Margue C, *et al.* Complete loss of PTEN expression as a possible early prognostic marker for prostate cancer metastasis. Int J Cancer 2007;120:1284–1292.
17 Yoshimoto M, Cunha IW, Coudry RA, *et al.* FISH analysis of 107 prostate cancers shows that PTEN genomic deletion is associated with poor clinical outcome. Br J Cancer 2007;97:678–685.
18 Tomlins SA, Mehra R, Rhodes DR, *et al.* TMPRSS2:ETV4 gene fusions define a third molecular subtype of prostate cancer. Cancer Res 2006;66: 3396–3400.
19 Perner S, Demichelis F, Beroukhim R, *et al.* TMPRSS2:ERG fusion-associated deletions provide insight into the heterogeneity of prostate cancer. Cancer Res 2006;66:8337–8341.
20 Cerveira N, Ribeiro FR, Peixoto A, *et al.* TMPRSS2-ERG gene fusion causing ERG overexpression precedes chromosome copy number changes in prostate carcinomas and paired HGPIN lesions. Neoplasia 2006;8:826–832.
21 Tomlins SA, Rhodes DR, Perner S, *et al.* Recurrent fusion of TMPRSS2 and ETS transcription factor genes in prostate cancer. Science 2005;310:644–648.
22 Wang J, Cai Y, Ren C, *et al.* Expression of variant TMPRSS2/ERG fusion messenger RNAs is associated with aggressive prostate cancer. Cancer Res 2006;66:8347–8351.
23 Ahlers CM, Figg WD. ETS-TMPRSS2 fusion gene products in prostate cancer. Cancer Biol Ther 2006;5:254–255.
24 Soller MJ, Isaksson M, Elfving P, *et al.* Confirmation of the high frequency of the TMPRSS2/ERG fusion gene in prostate cancer. Genes Chromosomes Cancer 2006; 45:717–719.
25 Rajput AB, Miller MA, De Luca A, *et al.* Frequency of the TMPRSS2:ERG gene fusion is increased in moderate to poorly differentiated prostate cancers. J Clin Pathol 2007;60:1238–1243.
26 Attard G, Clark J, Ambroisine L, *et al.* Duplication of the fusion of TMPRSS2 to ERG sequences identifies fatal human prostate cancer. Oncogene 2008;27:253–263.
27 Demichelis F, Fall K, Perner S, *et al.* TMPRSS2:ERG gene fusion associated with lethal prostate cancer in a watchful waiting cohort. Oncogene 2007;26:4596–4599.
28 Nami RK, Sugar L, Wang Z, *et al.* Expression of TMPRSS2:ERG gene fusion in prostate cancer cells is an important prognostic factor for cancer progression. Cancer Biol Ther 2007;6:40–45.
29 Winnes M, Lissbrant E, Damber JE, *et al.* Molecular genetic analyses of the TMPRSS2-ERG and TMPRSS2-ETV1 gene fusions in 50 cases of prostate cancer. Oncol Rep 2007;17:1033–1036.
30 Petrovics G, Liu A, Shaheduzzaman S, *et al.* Frequent overexpression of ETS-related gene-1 (ERG1) in prostate cancer transcriptome. Oncogene 2005;24: 3847–3852.
31 Yoshimoto M, Ludkovski O, Bayani J, *et al.* Microdeletion and concurrent translocation associated with a complex TMPRSS2:ERG prostate cancer gene fusion. Genes Chromosomes Cancer 2007;46:861–863.
32 Ventura RA, Martin-Subero JI, Jones M, *et al.* FISH analysis for the detection of lymphoma-associated chromosomal abnormalities in routine paraffin-embedded tissue. J Mol Diagn 2006;8:141–151.
33 Korshunov A, Sycheva R, Gorelyshev S, *et al.* Clinical utility of fluorescence *in situ* hybridization (FISH) in nonbrainstem glioblastomas of childhood. Mod Pathol 2005;18:1258–1263.
34 Kawai T, Hiroi S, Nakanishi K, *et al.* Abnormalities in chromosome 17 and p53 in lung carcinoma cells detected by fluorescence *in situ* hybridization. Pathol Int 2004;54:413–419.
35 Mezzelani A, Alasio L, Bartoli C, *et al.* c-erbB2/neu gene and chromosome 17 analysis in breast cancer by FISH on archival cytological fine-needle aspirates. Br J Cancer 1999;80:519–525.
36 Mehra R, Tomlins SA, Shen R, *et al.* Comprehensive assessment of TMPRSS2 and ETS family gene aberrations in clinically localized prostate cancer. Mod Pathol 2007;20:538–544.
37 Tomlins SA, Laxman B, Dhanasekaran SM, *et al.* Distinct classes of chromosomal rearrangements create oncogenic ETS gene fusions in prostate cancer. Nature 2007;448:595–599.
38 Tomlins SA, Laxman B, Varambally S, *et al.* Role of the TMPRSS2-ERG gene fusion in prostate cancer. Neoplasia 2008;10:177–188.
39 Gopalan A LM, Satagopan JM, Zhou QC, *et al.* 97th Annual Meeting of the United States and Canadian Academy of Pathology. The United States and Canadian Academy of Pathology: Denver, Colorado, 2008.
40 Hsu T, Trojanowska M, Watson DK. Ets proteins in biological control and cancer. J Cell Biochem 2004;91:896–903.
41 Shukla S, Maclennan GT, Hartman DJ, *et al.* Activation of PI3K-Akt signaling pathway promotes prostate cancer cell invasion. Int J Cancer 2007;121:1424–1432.
42 Kotelevets L, van Hengel J, Bruyneel E, *et al.* The lipid phosphatase activity of PTEN is critical for stabilizing intercellular junctions and reverting invasiveness. J Cell Biol 2001;155:1129–1135.
43 Larue L, Bellacosa A. Epithelial-mesenchymal transition in development and cancer: role of phosphatidylinositol 3′ kinase/AKT pathways. Oncogene 2005;24: 7443–7454.
44 Rhodes DR, Kalyana-Sundaram S, Mahavisno V, *et al.* Oncomine 3.0: genes, pathways, and networks in a collection of 18 000 cancer gene expression profiles. Neoplasia 2007;9:166–180.
45 Lapointe J, Li C, Higgins JP, *et al.* Gene expression profiling identifies clinically relevant subtypes of prostate cancer. Proc Natl Acad Sci USA 2004;101:811–816.
46 Glinsky GV, Glinskii AB, Stephenson AJ, *et al.* Gene expression profiling predicts clinical outcome of prostate cancer. J Clin Invest 2004;113:913–923.
47 Maira SM, Galetic I, Brazil DP, *et al.* Carboxyl-terminal modulator protein (CTMP), a negative regulator of PKB/Akt and v-Akt at the plasma membrane. Science 2001;294:374–380.
48 Polette M, Mestdagt M, Bindels S, *et al.* Beta-catenin and ZO-1: shuttle molecules involved in tumor invasion-associated epithelial-mesenchymal transition processes. Cells Tissues Organs 2007;185:61–65.